Alterations in Binding Site Density of Dopamine Transporter in the Striatum, Orbitofrontal Cortex, and Amygdala in Early Parkinson's Disease: Compartment Analysis for β-CFT Binding with Positron Emission Tomography

Yasuomi Ouchi, MD, PhD,* Etuji Yoshikawa, BA,† Hiroyuki Okada, BA,† Masami Futatsubashi, BA,† Yoshimoto Sekine, MD,‡ Masaomi Iyo, MD, PhD,‡ and Masanobu Sakamoto, MD, PhD§

We investigated changes in the kinetics in the binding of the dopamine transporter probe 2-β-carbomethoxy-3β-(4-[^{11}C]fluorophenyl)tropane (β-CFT) in living brain by compartmental analysis, using positron emission tomography in unmedicated patients with Parkinson's disease (PD) (Hoehn and Yahr stages I–II). With dynamic positron emission tomographic data from 90-minute acquisitions and metabolite-corrected arterial input functions, binding potentials (k_3/k_4) were calculated by using estimated rate constants ($K_1 - k_4$). In this analysis, the magnitude of the distribution volume (K_1/k_2) measured in the cerebellum, in which specific binding is negligible, was used as a constrained value for fitting in binding regions. Statistics showed that k_3/k_4 values in the striatum, the orbitofrontal cortex, and the amygdala were significantly lower in PD patients than in normal controls, whereas there were no differences in K_1/k_2 ratios and structural volumes between the groups. Correlation analysis showed that the putaminal and orbitofrontal binding levels were correlated positively with motor and mentation scores, respectively, of the Unified Parkinson's Disease Rating Scale. These results indicated that not only the striatal but also the orbitofrontal and amygdalar presynaptic dopaminergic functions were altered in early PD. The reductions in these mesocortical/mesolimbic functions might contribute to the mental and behavioral impairment observed in PD.

Ouchi Y, Yoshikawa E, Okada H, Futatsubashi M, Sekine Y, Iyo M, Sakamoto M. Alterations in binding site density of dopamine transporter in the striatum, orbitofrontal cortex, and amygdala in early Parkinson's disease: compartment analysis for β-CFT binding with positron emission tomography. Ann Neurol 1999;45:601–610

Quantitative analysis of the dopamine plasma membrane transporter permits examination of the functional integrity of dopaminergic innervation, because the transporter is located presynaptically on dopaminergic nerve terminals and transfers dopamine into presynaptic neurons.[1] Various positron-emitting ligands were developed for such imaging analysis in humans with positron emission tomography (PET), such as [^{11}C]nomifensine,[2] [^{18}F]GBR 13119,[3] [^{11}C]cocaine,[4] [^{11}C]WIN35,428 (CFT),[5–7] and [^{11}C]CIT.[8] It was reported that the phenyltropane analogues of cocaine, CFT and CIT, were more specific for dopamine uptake sites.[9] In vivo imaging with these high-affinity ligands is useful for detecting early alterations in presynaptic function in Parkinson's disease (PD). In these PET studies, however, the transporter activity was assessed by a qualitative method based on the relative radioactivity distribution in the brain. Wong and colleagues[5] used a four-parameter estimation model to calculate the transporter binding k_3/k_4 for WIN35,428 identical to CFT in baboon and human brains. Model-based analysis characterizes the brain regional response to an arterial input function and provides quantitative estimation of receptor binding parameters.[10] Unlike the qualitative ratio method, this approach allows separation of the radiotracer delivery from the binding

From the *Positron Medical Center and §Department of Neurology, Hamamatsu Medical Center, and ‡Department of Psychiatry, Hamamatsu Medical School, Hamamatsu; and †Central Research Laboratory, Hamamatsu Photonics KK, Hamakita, Japan.

Received Aug 3, 1998, and in revised form Dec 22. Accepted for publication Dec 22, 1998.

Address correspondence to Dr Ouchi, Positron Medical Center, Hamamatsu Medical Center, 5000 Hirakuchi, Hamakita 434-0041, Japan.

processes and can enhance our understanding of the PET results obtained from the brain in pathophysiological conditions such as PD.

Several imaging studies with PET or single-photon emission tomography demonstrated reductions in tissue uptake of [^{11}C]CIT,[8] ^{123}I-CIT,[11] and [^{11}C]CFT[9] in the striatum of patients with PD. This in vivo alteration in the striatal dopamine transporter was supported by the results of studies of PD post mortem that revealed that there were reductions in the dopamine transporter density[12] and the dopamine content[13] in the striatum, with relatively greater reduction in the putamen than in the caudate.[14] These PET studies were based chiefly on qualitative methods and dealt with PD patients with rather heterogeneous characteristics in terms of medication and clinical symptoms. This heterogeneity is common in a clinical setting and is occasionally enhanced by the concomitant incidence of mental abnormality. In addition, dopaminergic projections from the midbrain have been found in the orbital region of the prefrontal cortex and the amygdala.[15] Histological studies demonstrated severe neuronal loss in the amygdala in PD,[16] suggesting that the amygdalar or limbic dysfunction might be related to the development of mental and emotional alterations in PD patients.

The purpose of the present study was to quantitatively evaluate the density of the dopamine uptake sites in dopaminergic projection (mesocorticolimbic and nigrostriatal) regions by kinetic analysis based on a three-compartment, four-parameter model in normal subjects and early-PD patients. These parameters in each brain region were also compared with clinical scores in PD patients.

Subjects and Methods

Subjects and Patients

Six normal subjects (4 males and 2 females; mean age ± SD, 59.5 ± 3.8 years) and 8 age-matched unmedicated PD patients (4 males and 4 females; mean age, 63.1 ± 7.6 years) with a Hoehn and Yahr disability score[17] of 1 to 2 were examined. The severity of PD was assessed according to the Unified Parkinson's Disease Rating Scale (UPDRS).[18] In all patients, several neuropsychological tests were performed, including the Mini-Mental State Examination, the Wechsler Adult Intelligence Scale-Revised,[19] and paired verbal memory test. Patients were also assessed for depressive symptom severity with the Hamilton Depression Scale (HDS).[20] Neither patients nor normal subjects had medical treatment before the present PET study. L-Dopa treatment for all PD patients after the PET examination markedly ameliorated their parkinsonian symptoms. Patient characteristics are shown in Table 1. Magnetic resonance imaging (MRI) studies showed neither ischemic nor structural abnormalities in all participants. The present study was approved by the Ethics Committee of the Hamamatsu Medical Center and written informed consent was obtained from all participants.

MRI Procedure

To delineate the borders of the striatal nuclei, the orbital frontal cortex, and the amygdala in the placement of regions of interest (ROIs), MRI scanning was performed just before PET examination, using a static magnet (0.3 T MRP7000AD, Hitachi, Tokyo, Japan) with the following acquisition parameters: three-dimensional mode sampling; repetition time/echo time, 200 msec/23 msec; 75° flip angle; 2-mm slice thickness with no gap; and 256 × 256 matrices. The spatial relation between the center of magnetic field and that of PET images had been calibrated in advance. This calibration permitted us to perform quantitative PET scans set parallel to one MRI plane sectioned with an arbitrary angle such as the anterior–posterior commissure (AC-PC) plane or the hippocampal longitudinal axis plane by tilting the PET detector rings.[21] The shortage of the PET axial field of view obliged us to determine beforehand the PET scanning area that was covered from a middle portion of the cerebellum to a superior portion of the caudate on the midsagittal magnetic resonance (MR) image. The same rigid head fixation was performed by using a thermoplastic face mask designed for radiosurgical operation during both MRI and PET measurements.

Table 1. Details of Patient Characteristics

Patient No.	Age (yr)	Sex	DD	H&Y	MMSE	WAIS-R (v/p/t)	UPDRS (me/a/mo)	HDS	Paired Memory
1	64	M	1	1~2	28	85/78/81	5/8/20	14	7-7-8
2	65	M	0.4	1~2	25	125/111/119	2/3/14	7	9-10-10
3	47	M	0.5	1~2	29	97/98/97	2/4/20	8	7-8-9
4	72	M	0.3	2	26	88/84/85	3/5/17	10	7-8-8
5	63	F	5	2	27	81/82/81	7/11/13	15	6-7-7
6	71	F	2	1~2	27	98/93/95	3/5/19	9	8-8-9
7	62	F	1.2	2	24	84/78/80	10/10/21	23	6-6-7
8	64	F	1.5	2	27	99/86/93	7/11/26	14	8-8-9

DD = disease duration (yr); H&Y = Hoehn and Yahr disability score (1–5); MMSE = Mini-Mental State Examination (max = 30); WAIS-R = Wechsler Adult Intelligence Scale-Revised (v = verbal IQ; p = performance IQ; t = total IQ); UPDRS = Unified Parkinson's Disease Rating Scale (me = mentation, behavior, and mood; a = activities of daily living; mo = motor examination); HDS = Hamilton Depression Scale (reportedly, patients with mild depression would mark >14.7[57]); paired memory = verbal paired association test scoring numbers of word pairs that were relevant to each other in meaning and recalled on three successive trials (maximum score, 10/trial).

PET Procedure

We used a high-resolution brain PET scanner (SHR2400, Hamamatsu Photonics KK, Hamamatsu, Japan) with five detector rings yielding nine slice images simultaneously. The gantry of this tomograph could be tilted from −20° to +90°. The in-plane spatial resolution was 2.7 mm and the resolution in the axial plane was 5.5 mm full width at half maximum (FWHM) with an 80-mm axial field of view.[22] The gantry was set parallel to the intercommissural line determined by MRI[21] and a 20-minute transmission scan for attenuation correction was performed with a $^{68}Ge/^{68}Ga$ source. Then dynamic scanning began at the start of a slow bolus intravenous injection (taking 1 minute, through the right cubital vein) of a 450 MBq dose of β-CFT (time frames: 4 × 60 seconds, 20 × 120 seconds, and 14 × 300 seconds) followed by periodical arterial blood sampling from the left brachial artery for 90 minutes. PET images were reconstructed with a 6-mm Hanning filter (cutoff frequency, 0.2 cycles per pixel) as a 216 × 216 matrix image with a pixel size of 1.45 × 1.45 mm. Summation images constructed for each scan, using data collected 60 to 90 minutes after tracer injection, were used for the presentation as semiquantitative images normalized to the total radioactivity concentration in the cerebellum (standardized uptake ratio images).

Arterial Plasma Analysis

A total of 23 arterial blood samples were collected every 10 seconds for the first 1.5 minutes and at gradually longer intervals for the rest of the study. To determine unchanged radioligand and radioactive metabolites, additional arterial blood samples were drawn at 1, 5, 20, 30, and 45 minutes after injection of β-CFT. The metabolic transformation of radioligands was examined by measuring the fraction of radioactivity representing unchanged radioligand in plasma by using thin layer chromatography and a storage phosphor-screen bioimaging analyzer (BAS-1500, Fuji Film, Tokyo, Japan). The free metabolite–corrected plasma activities were fitted to a sum of three exponentials by the nonlinear least-squares method with the nonweighted Gauss–Newton algorithm.

Image Data Analysis

In the beginning, the MRI voxel size was adjusted to the PET voxel size three-dimensionally, using an image processing system (Dr View, Asahi Kasei Co, Tokyo, Japan)[21] on a SUN workstation (Hypersparc ss-20, SUN microsystems, CA). These reformatted MR images with three-dimensional scales and coordinates identical to the PET images were used as an anatomical reference for the following PET ROI analysis. The ROI setting was chiefly performed by two technologists who were not informed of the subject's diagnosis. Irregular ROIs larger than 2 full width at half maximum (FWHM) (in each dimension), which could minimize the influence of the partial volume effects,[23] were drawn bilaterally over the caudate, putamen, orbitofrontal cortex, amygdala, and cerebellum (Fig 1) on the MR images, according to the human brain atlas.[24] To investigate the partial volume effects on the PET results, we performed a volumetric study of each brain structure by calculating the product of the

Fig 1. Region of interest (ROI) setting. Irregular ROIs, drawn bilaterally on the concerned regions on the magnetic resonance images (upper row), were placed on the corresponding positron emission tomographic images (bottom row). Ce = *cerebellum;* A = *amygdala;* O = *orbitofrontal cortex;* Cd = *caudate;* P = *putamen.*

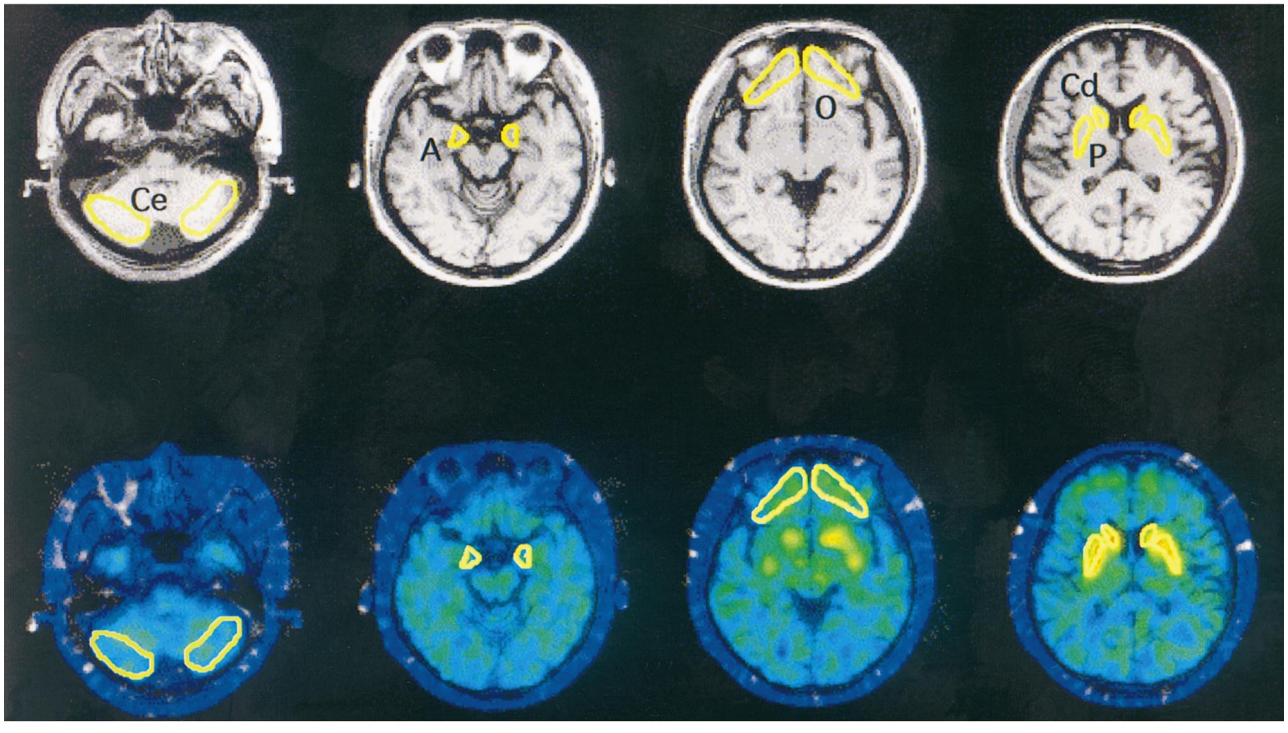

semicircular area drawn on the MRI scan and the slice thickness. The amygdala occupies the superomedial protrusion part of the uncus. Although the boundaries between the amygdala and the medial border of the amygdala connecting to the entorhinal cortex, and between the amygdala and the anterior segment of the hippocampal head were difficult to detect on the images parallel to the bicommissural line, in the current study the amygdalar ROI was considered to cover most of the amygdala and parts of the neighboring cortical area.[25] The border of the orbital frontal cortex was outlined in the prefrontal region from the rectus gyrus to the bottom of the genu of the corpus callosum.[24,26] The borders for the caudate and putamen were delineated on all planes on which they appeared.[27] After delineation of the ROIs was completed on the reformatted MR images, PET images were displayed side-by-side together with the MR images. Then, the determined ROIs were placed on the same area on both the MR and the corresponding PET images. Both reconstructed PET and MRI images were obtained parallel to the intercommissural line so that they theoretically required no reorientation procedure. However, in some cases in which head motion occurred during scanning, PET images had to be rearranged on their sagittal views by visual inspection, using the imaging software. As the amygdala is approximately 1.6 cm^3 in volume,[28] one PET image, which integrated data of 6.5-mm thickness[22] as a volume of radioactivity, contained the functional information of the amygdala at least 6.5 mm deep in the z direction. Thus, we regarded the ROI value on a single PET image as a regional (volume) value of ligand uptake in the present study.

As shown in the model (Fig 2) used in the present study, the three compartments are composed of plasma, free and nonspecifically bound ligand in the brain, and specifically bound ligand in the brain.[5] Data were analyzed based on this three-compartment, four-parameter model, fitting for blood–brain barrier transport rates (K_1), the free + nonspecific distribution volume (K_1/k_2), and the binding and dissociation rate constants (k_3 and k_4, respectively).[5,29] First, the distribution volume K_1/k_2 was fitted to the cerebellum, which was assumed to be an appropriate region for estimation of nonspecific binding because it contains negligible dopamine concentrations and dopamine receptors.[30] The time–activity curves were corrected for the presence of the vascular compartment, which was fixed to a value of 3.5% of brain volume.[29] On the assumption that the ratio K_1/k_2 in the cerebellum was the same in other parts of the brain including the striatum, the rate constants K_1, k_3, and k_4 in the concerned brain regions were measured by fitting the metabolite-corrected plasma time–radioactivity curves of β-CFT and cerebral blood volume–corrected brain time–activity curves, using a nonlinear least-squares algorithm. The measure of transporter binding was regarded as the k_3/k_4 ratio in the region concerned. Because, biochemically, $k_3 = k_{on} \cdot B_{max}'$ (k_{on} = biomolecular association rate between ligand and receptor; B_{max}' = receptor density of unoccupied receptors), $k_4 = k_{off}$ (k_{off} = dissociation rate of ligand from the receptor complex), and $k_d = k_{off}/k_{on}$, the ratio k_3/k_4 is equivalent to B_{max}'/k_d, which has been referred to as binding potential.[31] These rate constants and binding potentials were the final estimates to be compared for evaluation of the function of the dopamine transporter in the present study.

Fig 2. Three-compartment model for describing β-CFT kinetics in this study. The second compartment (Qf+Ns) is combined from free and nonspecific pools in the six-parameter model into a single compartment to reduce the number of parameters to four. Under these conditions, rate constants k_5 *and* k_6 *(forward and backward rates to Ns, respectively) are assumed to be rapid compared with blood–brain barrier transport rates* (K_1 *and* k_2). *The values* k_3 *and* k_4 *are the forward and reverse transport rate constants to the specific binding compartment (Qs), respectively.* C_p = *β-CFT concentration in plasma.*

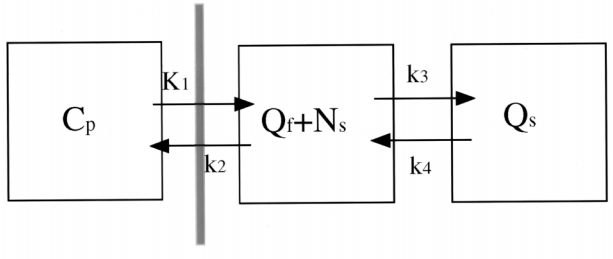

Statistics

As there was no significant difference in age between PD and normal control subjects ($p > 0.05$, χ^2 test), the PET results were not corrected for age as a confounding effect before statistical analysis. Rate constants and binding levels were first assessed by two-way analysis of variance (ANOVA) with post hoc Scheffé's F test with respect to one between-subject factor (PD, normal control) and within-subject factor (striatal region consisting of the caudate and putamen bilaterally after values from these regions were averaged as a value of the striatal area, and extrastriatal region consisting of the amygdala and orbitofrontal cortex bilaterally) to evaluate the level of the estimates' reduction in the extrastriatal region because of lower dopamine binding site. Then, because no cross-interaction was observed in two-way ANOVA between the locations (striatal or extrastriatal regions and types of diagnosis), one-way ANOVA was preformed to compare all estimates including the hemispheric side in either region separately. Because post hoc multiple comparisons were performed in these analyses, statistical significance was set at $p < 0.05$. Statistical analysis for volume was performed by using one-way ANOVA with post hoc Scheffé's F test. In addition, correlation coefficients were calculated for the binding levels and neuropsychometric scores in PD patients, using Pearson's rank correlation analysis. The level of significance was $p < 0.05$.

Results

Patient Characteristics

Intelligence scores showed that none of the PD patients were clinically demented. UPDRS subscores for mentation and HDS reflected mild depression in half of the PD patients. However, these mentation scores were not correlated with the Hoehn and Yahr severity

score or UPDRS motor subscore ($p > 0.05$, Spearman rank correlation.

β-CFT Binding in the Striatal and Extrastriatal Regions in Normal Subjects and PD Patients

The time–activity curves of β-CFT are shown in Figure 3. After administration of β-CFT, radioactivity accumulated gradually in the striatum (putamen), and also to a lesser extent in the orbitofrontal cortex in normal subjects. The amygdalar radioactivity concentration rapidly reached a plateau. In contrast, the putaminal radioactivity in PD patients did not increase with time, and the orbitofrontal and amygdalar β-CFT accumulation showed a gradual decrease after reaching a peak. The pattern of time–activity curves of the metabolite-corrected plasma and cerebellum showed no differences between the two groups. This was confirmed by the observation that the distribution volume K_1/k_2 in the cerebellum was almost the same between the two groups (Table 2). Statistical analysis of the results of kinetic studies of β-CFT binding showed that the levels of B_{max}'/k_d (k_3/k_4) in the striatum and the orbitofrontal and amygdalar regions in PD group were significantly lower than those in the age-matched normal group. The value k_3/k_4 in the putamen contralateral to the affected side in PD patients was markedly reduced. Because of a large standard deviation in k_3 value, the post hoc F test failed to detect a significant difference in k_3 between the two groups. K_1 values in all areas examined also showed no differences between the patients and control subjects. There was no significant difference in volumes of all structures involved between PD patients and normal subjects (Table 3).

Correlation Between Neuropsychometric Scores and Regional β-CFT Binding

Regression analysis showed significant negative correlations between HDS score and β-CFT binding (k_3/k_4) in the orbitofrontal cortex (Fig 4A; $R^2 = 0.65$, $p < 0.03$), between mentation scores of UPDRS and the orbitofrontal k_3/k_4 level (see Fig 4B; $R^2 = 0.674$, $p < 0.02$), and between motor scores of UPDRS and the putaminal k_3/k_4 level (see Fig 4C; ipsilateral: $R^2 = 0.743$, contralateral: $R^2 = 0.652$, $p < 0.02$). No significant correlation was observed between UPDRS scores and amygdalar β-CFT binding.

Discussion

This β-CFT PET study was focused on in vivo quantitative measurement of dopamine transporter activities in the striatal and the extrastriatal dopaminergic projection regions in PD patients, based on kinetic modeling with arterial plasma sampling. To our knowledge, this is the first investigation of dopamine transporter binding in the mesolimbic and mesocortical projection regions in L-dopa–naive PD patients. The major find-

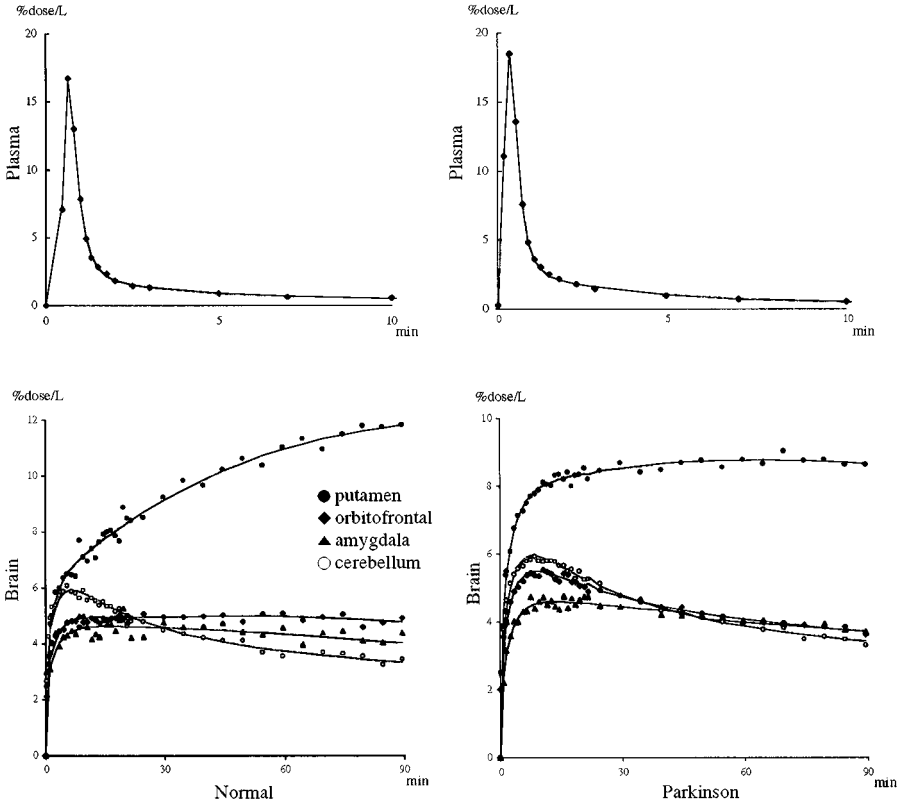

Fig 3. Time–activity curves of the metabolite-corrected radioactivity in the plasma and the regional brain radioactivities of a normal subject and a parkinsonian patient after injection of β-CFT.

Table 2. Kinetic Parameters for [^{11}C]β-CFT in Brain Regions of PD Patients and Normal Controls (mean ± SD)

Group		Cerebellum		Caudate Ipsi	Caudate Contra	Putamen Ipsi	Putamen Contra	Amygdala Ipsi	Amygdala Contra	Orbitofrontal (Bilateral)
Normal	K_1	0.443 ± 0.074	K_1	0.415 ± 0.115	0.426 ± 0.092	0.465 ± 0.108	0.474 ± 0.101	0.312 ± 0.058	0.347 ± 0.033	0.378 ± 0.85
	k_2	0.058 ± 0.010	k_2	0.055 ± 0.010	0.056 ± 0.010	0.061 ± 0.009	0.063 ± 0.009	0.041 ± 0.007	0.047 ± 0.007	0.051 ± 0.010
	K_1/k_2	7.654 ± 1.153	k_3	0.495 ± 0.283	0.442 ± 0.237	0.393 ± 0.252	0.454 ± 0.277	0.067 ± 0.058	0.062 ± 0.043	0.062 ± 0.048
			k_4	0.116 ± 0.065	0.103 ± 0.054	0.092 ± 0.067	0.112 ± 0.071	0.350 ± 0.311	0.290 ± 0.245	0.374 ± 0.266
			k_3/k_4	4.184 ± 0.712	4.207 ± 0.599	4.176 ± 0.566	4.012 ± 0.537	0.193 ± 0.051	0.231 ± 0.055	0.190 ± 0.088
PD	K_1	0.411 ± 0.065	K_1	0.434 ± 0.079	0.426 ± 0.047	0.445 ± 0.238	0.458 ± 0.054	0.328 ± 0.215	0.315 ± 0.065	0.352 ± 0.080
	k_2	0.051 ± 0.012	k_2	0.054 ± 0.012	0.053 ± 0.008	0.056 ± 0.009	0.056 ± 0.009	0.039 ± 0.012	0.041 ± 0.015	0.044 ± 0.007
	K_1/k_2	7.898 ± 0.742	k_3	0.218 ± 0.142	0.240 ± 0.175	0.091 ± 0.059	0.202 ± 0.132	0.016 ± 0.040	0.019 ± 0.011	0.007 ± 0.004
			k_4	0.104 ± 0.076	0.129 ± 0.104	0.076 ± 0.031	0.213 ± 0.208	0.141 ± 0.126	0.124 ± 0.117	0.075 ± 0.047
			k_3/k_4	2.244[a]± 0.420	1.961[a]± 0.301	1.284[a]± 0.539	1.069[a]± 0.536	0.106[a]± 0.077	0.144[a]± 0.053	0.098[a]± 0.022

Values for K_1 are given as ml mg^{-1} min^{-1} and for k_2–k_4 in min^{-1}.

[a] $p < 0.05$ vs control group.

[^{11}C]β-CFT = 2-β-carbomethoxy-3β-(4-[^{11}C]fluorophenyl) tropane; PD = Parkinson's disease; Ipsi = ipsilateral; Contra = contralateral.

Table 3. MRI-Defined Volumes of the Brain Structures

Region	Side	Normal	PD
Caudate	Right	1.80 ± 0.38	1.73 ± 0.55
	Left	1.88 ± 0.46	1.78 ± 0.62
Putamen	Right	2.53 ± 0.12	2.41 ± 0.13
	Left	2.50 ± 0.70	2.48 ± 0.93
Amygdala	Right	1.97 ± 0.72	1.88 ± 0.42
	Left	1.98 ± 0.66	1.87 ± 0.48
Orbitofrontal cortex	Bilateral	14.9 ± 0.4	14.1 ± 0.6

Data are given as mean ± SD and are expressed as cubic centimeters.

There were no significant differences between groups ($p > 0.05$, one-way analysis of variance).

MRI = magnetic resonance imaging; PD = Parkinson's disease.

ing was parallel reductions in the binding levels in these extrastriatal regions along with reduction in the striatal binding in PD. Three-compartment analysis indicated a k_3/k_4 value in the normal striatum close to 4, which was consistent with the results of a previous PET study with [^{11}C]WIN 35,248[5] showing a value on the order of 4 to 5. The slight decrease in magnitude in our study might have been caused by a methodological difference in measuring the amount of metabolite (<10% by thin layer chromatography vs <20% by high performance liquid chromatography), because such a decrease was shown to reduce the k_3/k_4 level.[5] Wide variations in both k_3 and k_4 estimates in the present study indicated that these two parameters were not exclusively identifiable. This might have been because that equilibration between the bound and free ligand compartments occurred too rapidly to differentiate these two compartments kinetically with much certainty.[29] The advantage of estimating B_{max}'/k_d (k_3/k_4) is that the ratio of the two parameters is considerably stable even in low receptor density regions such as the orbitofrontal cortex and the amygdala. This was in agreement with a previous compartment analysis study with [^{11}C]flumazenil indicating that a three-compartment model yielded the best fit for estimating B_{max}'/k_d in regions of low receptor density.[29] With this B_{max}'/k_d approach, B_{max}'/k_d (k_3/k_4) values in both striatal and extrastriatal dopaminergic projection regions were found to be significantly lower in PD patients than in normal subjects in the present study. This result demonstrated that not only nigrostriatal but also mesocortical/mesolimbic presynaptic dopamine functions are substantially altered in patients with early PD.

The reduction of β-CFT binding in the striatum in the present study is in accord with previous reports of dopamine transporter imaging studies, using a striatum–cerebellum ratio method,[8,9,11] which revealed a significant reduction in the striatal uptake. Specifically, the putaminal reduction in the β-CFT binding was more prominent in the present study, which is in agreement with the results from [^{18}F]dopa studies[32–34] and dopamine transporter PET studies indicating 56 to 80% reductions in putaminal uptake.[35,36] Although we did not divide the putamen in the anteroposterior direction, all β-CFT images in PD patients illustrated lower accumulation of the radiocompound in the posterior portion of the putamen (Fig 5). The relatively greater reduction in this index of the density of dopamine uptake sites is in agreement with the results of pathological studies showing that the decline in dopamine level was greater in the posterior versus the anterior putamen.[14] This might reflect severe loss of dopaminergic neurons in the ventrolateral substantia nigra projecting chiefly to the posterior putamen in contrast to the rostral and medial neurons projecting primarily to the caudate nucleus.[14,37,38]

It is noteworthy that β-CFT binding in the orbital portion of the prefrontal cortex and the amygdala was also decreased in PD at Hoehn and Yahr stage 2 in the present study. Histologically, the prefrontal cortical region is innervated by both the ventral tegmental area and the dorsal tier of the substantia nigra com-

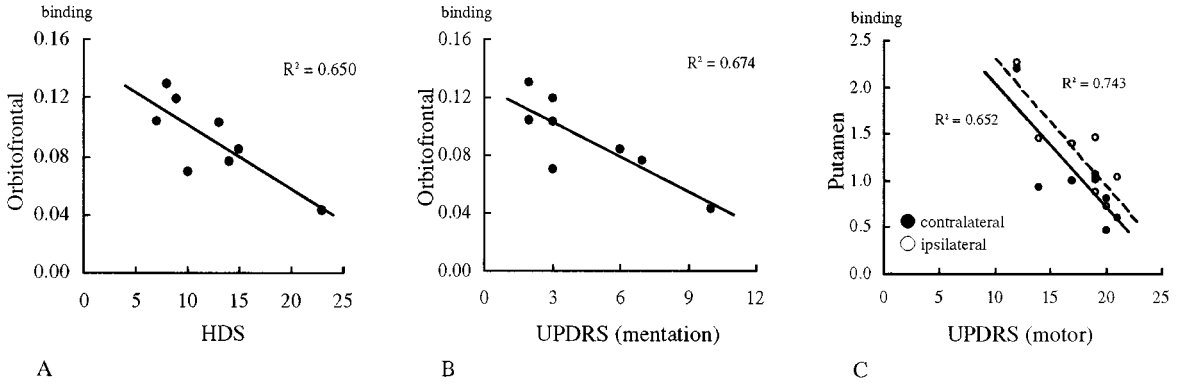

Fig 4. Correlation of neuropsychometric scores with regional k_3/k_4 values for Parkinson's disease patients. (A) Orbitofrontal binding versus Hamilton Depression Scale (HDS) score. (B) Orbitofrontal binding versus mentation scores of Unified Parkinson's Disease Rating Scale (UPDRS). (C) Putaminal binding versus motor scores of UPDRS.

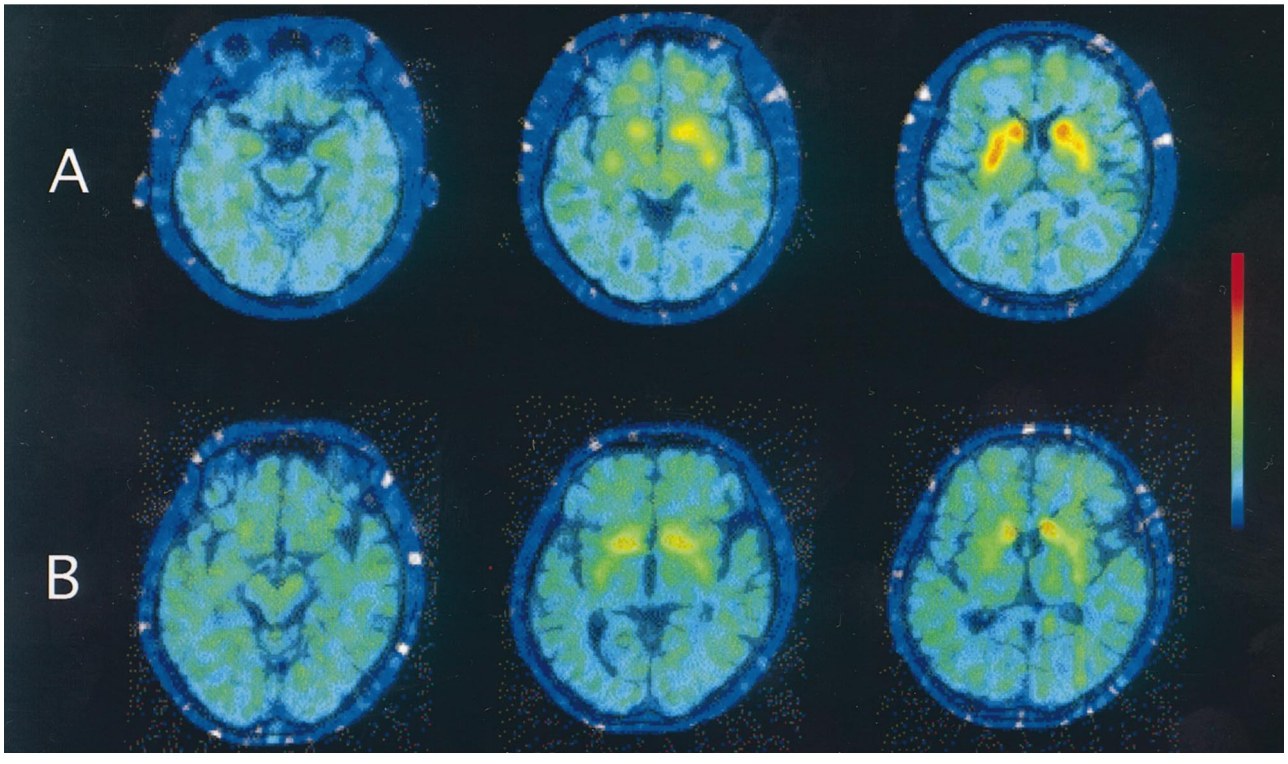

Fig 5. Transaxial positron emission tomographic images of β-CFT activity superimposed on magnetic resonance images, accumulated 60 to 90 minutes after tracer injection and normalized to the cerebellar activity, for a normal subject (A) and a Parkinson's disease (PD) patient (B) with a Hoehn and Yahr severity of grade 2. The image for the normal subject shows a mild increase in β-CFT uptake in the orbital portion of the prefrontal cortex and the amygdalar region, in contrast to the image for the PD patient. Marked reduction in β-CFT uptake was found in the bilateral putamen of the PD brain. The color bar indicates the normalized count from 0 to 90 Bq/ml.

pacta.[39,40] Postmortem studies showed a 42% reduction in number of ventral tegmental neurons and significant decreases in dopamine levels in the frontal cortex and hippocampus in PD patients,[41,42] and loss of 40 to 60% of cells in the ventral tegmental area.[43] This neuronal loss was similar to our result showing a 48% reduction in k_3/k_4 level in the orbitofrontal cortex of PD patients compared with normal subjects. Reduction of approximately 30 to 45% of binding was found in the amygdala of PD patients, which was supported by the results of the pathological analyses showing that the pathological changes including Lewy bodies and Lewy neurites oc-

curred prominently in the accessory cortical and central nuclei of the amygdala in PD.[16,44] In humans, amygdalar lesions that spare the hippocampus do not grossly affect memory or intelligence, but do impair reactivation of remembered and emotionally significant events.[45] Recent imaging studies have provided evidence of amygdalar function in processing of emotional learning[46,47] and emotional facial recognition.[48–50] In PD without dementia, this emotional facial expression and recognition of others is deteriorated.[51] Thus, we speculate that insufficiency of mesolimbic dopamine leading to amygdalar hypoactivity may alter normal processing for emotional expression and recognition in PD.

Correlation analysis between psychometric scores and regional β-CFT binding showed that motor UPRDS was significantly correlated with bilateral putaminal binding measures, in accord with studies using [^{18}F]dopa uptake[52] and [^{123}I]β-CIT uptake[11] showing that the putaminal uptakes of these ligands were highly correlated with motor UPDRS, specifically, with a subscore for bradykinesia. Of interest is the significant correlation of the binding k_3/k_4 in the orbitofrontal cortex with mentation UPDRS and HDS scores in PD observed in the present study. Considering that the orbitofrontal binding of β-CFT was reduced in PD, this negative correlation strengthens the conjecture that the mesocortical hypofunction is responsible for the lack of mental activation in PD. The poor correlation of the amygdalar binding with mentation UPDRS score was not surprising given that the scores were within normal limits for intelligence and memory in the PD group. Furthermore, mentation UPDRS and HDS scores are not satisfactory indices of emotional state. PET scans parallel to the hippocampal longitudinal axis plane can provide metabolic information in the hippocampus.[53] In contrast, scans parallel to the bicommissural line performed in the present study did not allow us to demarcate the hippocampus entirely, so that the hippocampal binding of β-CFT was not investigated. However, based on the observed reduction in ligand binding in the amygdala, we suspect that the hippocampus, if it could be resolved, might also be affected in PD, as suggested in a previous pathological study.[44]

The present findings must be viewed considering several possible problems. First, the risk of placing small ROIs on tomographic images irrespective of using a high-resolution PET scanner may result in the partial volume effect. Amygdala and caudate ROIs were smaller in volume than were the other ROIs. Our MRI-based volumetric study showed no significant difference in volumes of all structures between PD patients and normal subjects (see Table 3), in accord with the results from the previous volumetric studies.[26,27,53] The significant differences in the tracer binding in regions identified as containing the striatum or the amygdala or the orbitofrontal cortex cannot be attributed to effects of partial volume, as volumes were identical in both groups. Second, there is an age-related reduction in the concentration of dopamine transporters as a function of normal aging, which is reported to decline at a rate of 4.5% per decade.[54] In the present study, there was no significant difference in age between the two groups (normal and PD) and no age-related reduction in striatal β-CFT binding (not shown) possibly because of the narrow age range, with most subjects in their fifties and sixties. These findings permitted further analyses without considering age-related effects. Third, chronic or acute treatment with antiparkinsonian medication can be a confounding factor in the interpretation of inconsistencies,[55] but our PD patients were all free from medication at the time of PET examination. Marked improvement of parkinsonism by L-dopa treatment after the PET study confirmed that all patients were parkinsonian. Finally, it may be uncertain whether this decrease in binding was because of a decrease in presynaptic dopamine terminals or a decrease in dopamine transporter availability, because it was reported that the level of messenger RNA for the dopamine transporter in the substantia nigra declined more rapidly with age than the number of nigral neurons.[56] However, the pathological evidences on PD brain,[12,13] and the present decrease in β-CFT binding in PD patients with the same age as normal subjects, suggested that this reduction in binding was caused by the loss of nigral and ventral tegmental neurons in PD.

In conclusion, our kinetic and neuropsychometric study indicated that not only nigrostriatal but also mesocortical/mesolimbic dopaminergic systems are affected at the early stage of PD, and the latter dysfunctions may contribute to the mental impairment seen in PD patients.

We thank Shuji Nobezawa, Toshihiko Kanno, Dr Tatsuo Torizuka (Hamamatsu Medical Center), and Dr Koichi Ishizu (Fukui Medical School) for their technical support, as well as Dr Hideo Tsukada (Hamamatsu Photonics KK) for his help in performing our PET experiment.

References

1. Kuhar MJ, Sanchez-Roa PM, Wong DF, et al. Dopamine transporter: biochemistry, pharmacology and imaging. Eur Neurol 1990;30:15–20
2. Aquilonius SM, Bergstrom K, Eckernas SA, et al. In vivo evaluation of striatal dopamine reuptake sites using 11C-nomifensine and positron emission tomography. Acta Neurol Scand 1987;76:283–287
3. Kilbourn MR. In vivo binding of [18F]GBR 13119 to the brain dopamine uptake system. Life Sci 1988;42:1347–1353
4. Fowler JS, Volkow ND, Wolf AP, et al. Mapping cocaine binding sites in human and baboon brain in vivo. Synapse 1989;4:371–377
5. Wong DF, Yung B, Dannals RF, et al. In vivo imaging of ba-

boon and human dopamine transporters by positron emission tomography using [^{11}C]WIN 35,428. Synapse 1993;15:130–142
6. Wullner U, Pakzaban P, Brownell AL, et al. Dopamine terminal loss and onset of motor symptoms in MPTP-treated monkeys: a positron emission tomography study with ^{11}C-CFT. Exp Neurol 1994;126:305–309
7. Villemagne V, Yuan J, Wong DF, et al. Brain dopamine neurotoxicity in baboons treated with doses of methamphetamine comparable to those recreationally abused by humans: evidence from [^{11}C]WIN-35,428 positron emission tomography studies and direct in vitro determinations. J Neurosci 1998;18:419–427
8. Laihinen AO, Rinne JO, Nagren KA, et al. PET studies on brain monoamine transporters with carbon-11-beta-CIT in Parkinson's disease. J Nucl Med 1995;36:1263–1267
9. Rinne JO, Laihinen A, Nagren K, et al. PET examination of the monoamine transporter with [^{11}C]beta-CIT and [11C]beta-CFT in early Parkinson's disease. Synapse 1995;21:97–103
10. Gjedde A, Wong DF. Modeling neuroreceptor binding of radioligands in vivo. In: Frost JJ, Wagner HR Jr, eds. Quantitative imaging: neuroreceptors, neurotransmitters, and enzymes. New York: Raven Press, 1990:51–79
11. Seibyl JP, Marek KL, Quinlan D, et al. Decreased single-photon emission computed tomographic [^{123}I]β-CIT striatal uptake correlates with symptom severity in Parkinson's disease. Ann Neurol 1995;38:589–598
12. Kaufman MJ, Madras BK. Severe depletion of cocaine recognition sites associated with the dopamine transporter in Parkinson's-diseased striatum. Synapse 1991;9:43–49
13. Bernheimer H, Birkmayer W, Hornykiewicz O, et al. Brain dopamine and the syndromes of Parkinson and Huntington. Clinical, morphological and neurochemical correlations. J Neurol Sci 1973;20:415–455
14. Kish SJ, Shannak K, Hornykiewicz O. Uneven pattern of dopamine loss in the striatum of patients with idiopathic Parkinson's disease. Pathophysiologic and clinical implications. N Engl J Med 1988;318:876–880
15. Oades RD, Halliday GM. Ventral tegmental (A10) system: neurobiology. 1. Anatomy and connectivity. Brain Res 1987; 434:117–165
16. Braak H, Braak E, Yilmazer D, et al. Amygdala pathology in Parkinson's disease. Acta Neuropathol Berl 1994;88:493–500
17. Hoehn MW, Yahr MD. Parkinsonism: onset, progression, and mortality. Neurology (Minneap) 1967;17:427–445
18. Fahn S, Elton RL. Unified Parkinson's disease rating scale. In: Fahn S, Marsden CD, Calne DB, Goldstein M, eds. Recent developments in Parkinson's disease. Florham Park, NJ: MacMillan Healthcare Information, 1987:153–163
19. Wechsler D. The Wechsler adult intelligence scale-revised. San Antonio, TX: Psychological Corporation, 1981
20. Hamilton M. A rating scale for depression. J Neurol Neurosurg Psychiatry 1960;23:56–62
21. Ouchi Y, Nobezawa S, Okada H, et al. Glucose metabolism of the human hippocampal formation in the hippocampal long axis plane measured by PET. J Cereb Blood Flow Metab 1997; 17:S218 (Abstract)
22. Yamashita T, Uchida H, Okada H, et al. Development of a high resolution PET. IEEE Trans Nucl Sci 1990;37:594–599
23. Hoffman E, Phelps M. Positron emission tomography: principles and quantification. In: Phelps M, Mazziotta JC, Schelbert HR, eds. Positron emission tomography and autoradiography: principles and applications for the brain and heart. New York: Raven Press, 1986:237–286
24. Mai JK, Assheuer J, Paxinos G. Atlas of the human brain. San Diego: Academic Press, 1997
25. Watson C, Andermann F, Gloor P, et al. Anatomic basis of amygdaloid and hippocampal volume measurement by magnetic resonance imaging. Neurology 1992;42:1743–1750
26. Buchanan RW, Vladar K, Barta PE, Pearlson GD. Structural evaluation of the prefrontal cortex in schizophrenia. Am J Psychiatry 1998;155:1049–1055
27. Backman L, Robins-Wahlin TB, Lundin A, et al. Cognitive deficits in Huntington's disease are predicted by dopaminergic PET markers and brain volumes. Brain 1997;120:2207–2217
28. Soininen HS, Partanen K, Pitkanen A, et al. Volumetric MRI analysis of the amygdala and the hippocampus in subjects with age-associated memory impairment: correlation to visual and verbal memory. Neurology 1994;44:1660–1668
29. Koeppe RA, Holthoff VA, Frey KA, et al. Compartmental analysis of [11C]flumazenil kinetics for the estimation of ligand transport rate and receptor distribution using positron emission tomography. J Cereb Blood Flow Metab 1991;11:735–744
30. Palacios JM, Camps M, Cortes R, Probst A. Mapping dopamine receptors in the human brain. J Neural Transm Suppl 1988;27:227–235
31. Mintun MA, Raichle ME, Kilbourn MR, et al. A quantitative model for the in vivo assessment of drug binding sites with positron emission tomography. Ann Neurol 1984;15:217–227
32. Brooks DJ, Ibanez V, Sawle GV, et al. Differing patterns of striatal [^{18}F]dopa uptake in Parkinson's disease, multiple system atrophy, and progressive supranuclear palsy. Ann Neurol 1990; 28:547–555
33. Burn DJ, Mark MH, Playford ED, et al. Parkinson's disease in twins studied with ^{18}F-dopa and positron emission tomography. Neurology 1992;42:1894–1900
34. Cumming P, Gjedde A. Compartmental analysis of dopa decarboxylation in living brain from dynamic positron emission tomograms. Synapse 1998;29:37–61
35. Frost JJ, Rosier AJ, Reich SG, et al. Positron emission tomographic imaging of the dopamine transporter with ^{11}C-WIN 35,428 reveals marked declines in mild Parkinson's disease. Ann Neurol 1993;34:423–431
36. Guttman M, Burkholder J, Kish SJ, et al. [^{11}C]RTI-32 PET studies of the dopamine transporter in early dopa-naive Parkinson's disease: implications for the symptomatic threshold. Neurology 1997;48:1578–1583
37. Rinne JO, Rummukainen J, Paljarvi L, Rinne UK. Dementia in Parkinson's disease is related to neuronal loss in the medial substantia nigra. Ann Neurol 1989;26:47–50
38. Fearnley JM, Lees AJ. Ageing and Parkinson's disease: substantia nigra regional selectivity. Brain 1991;114:2283–2301
39. Porrino LJ, Goldman-Rakic PS. Brain stem innervation of prefrontal and anterior cingulate cortex in the rhesus monkey revealed by retrograde transport of HRP. J Comp Neurol 1982; 205:63–76
40. Oeth KM, Lewis DA. Cholecystokinin- and dopamine-containing mesencephalic neurons provide distinct projections to monkey prefrontal cortex. Neurosci Lett 1992;145:87–92
41. Scatton B, Rouquier L, Javoy-Agid F, Agid Y. Dopamine deficiency in the cerebral cortex in Parkinson disease. Neurology 1982;32:1039–1040
42. German DC, Manaye K, Smith WK, et al. Midbrain dopaminergic cell loss in Parkinson's disease: computer visualization. Ann Neurol 1989;26:507–514
43. Uhl GR, Hedreen JC, Price DL. Parkinson's disease: loss of neurons from the ventral tegmental area contralateral to therapeutic surgical lesions. Neurology 1985;35:1215–1218
44. Churchyard A, Lees AJ. The relationship between dementia and direct involvement of the hippocampus and amygdala in Parkinson's disease. Neurology 1997;49:1570–1576
45. Sarter M, Markowitsch HJ. The amygdala's role in human mnemonic processing. Cortex 1985;21:7–24
46. LaBar KS, Gatenby JC, Gore JC, et al. Human amygdala acti-

vation during conditioned fear acquisition and extinction: a mixed-trial fMRI study. Neuron 1998;20:937–945
47. Morris JS, Ohman A, Dolan RJ. Conscious and unconscious emotional learning in the human amygdala. Nature 1998;393: 467–470
48. Adolphs R, Tranel D, Damasio H, Damasio AR. Fear and the human amygdala. J Neurosci 1995;15:5879–5891
49. Phillips ML, Young AW, Senior C, et al. A specific neural substrate for perceiving facial expressions of disgust. Nature 1997; 389:495–498
50. Morris JS, Friston KJ, Buchel C, et al. A neuromodulatory role for the human amygdala in processing emotional facial expressions. Brain 1998;121:47–57
51. Jacobs DH, Shuren J, Bowers D, Heilman KM. Emotional facial imagery, perception, and expression in Parkinson's disease. Neurology 1995;45:1696–1702
52. Eidelberg D, Moeller JR, Dhawan V, et al. The metabolic anatomy of Parkinson's disease: complementary [^{18}F]fluorodeoxyglucose and [^{18}F]fluorodopa positron emission tomographic studies. Mov Disord 1990;5:203–213
53. Ouchi Y, Nobezawa S, Okada H, et al. Altered glucose metabolism in the hippocampal head in memory impairment. Neurology 1998;51:136–142
54. Rinne JO, Sahlberg N, Ruottinen H, et al. Striatal uptake of the dopamine reuptake ligand [^{11}C]beta-CFT is reduced in Alzheimer's disease assessed by positron emission tomography. Neurology 1998;50:152–156
55. Torstenson R, Hartvig P, Langstrom B, et al. Differential effects of levodopa on dopaminergic function in early and advanced Parkinson's disease. Ann Neurol 1997;41:334–340
56. Bannon MJ, Poosch MS, Xia Y, et al. Dopamine transporter mRNA content in human substantia nigra decreases precipitously with age. Proc Natl Acad Sci USA 1992;89:7095–7099
57. Carroll BJ, Feinberg M, Smouse PE, et al. The Carroll rating scale for depression. I. Development, reliability and validation. Br J Psychiatry 1981;138:194–200